

# Green Chemistry

Accepted Manuscript



This article can be cited before page numbers have been issued, to do this please use: S. Li, Y. Wang, Y. Yang, B. Chen, J. Tai, H. Liu and B. Han, *Green Chem.*, 2019, DOI: 10.1039/C8GC03529F.



This is an Accepted Manuscript, which has been through the Royal Society of Chemistry peer review process and has been accepted for publication.

Accepted Manuscripts are published online shortly after acceptance, before technical editing, formatting and proof reading. Using this free service, authors can make their results available to the community, in citable form, before we publish the edited article. We will replace this Accepted Manuscript with the edited and formatted Advance Article as soon as it is available.

You can find more information about Accepted Manuscripts in the [author guidelines](#).

Please note that technical editing may introduce minor changes to the text and/or graphics, which may alter content. The journal's standard [Terms & Conditions](#) and the ethical guidelines, outlined in our [author and reviewer resource centre](#), still apply. In no event shall the Royal Society of Chemistry be held responsible for any errors or omissions in this Accepted Manuscript or any consequences arising from the use of any information it contains.

Journal Name

COMMUNICATION

## Conversion of levulinic acid to $\gamma$ -valerolactone over ultra-thin TiO<sub>2</sub> nanosheets decorated with ultrasmall Ru nanoparticle catalysts under mild condition

rReceived 00th January 20xx,  
Accepted 00th January 20xx

DOI:  
10.1039/x0xx00000xwww.rsc.org/

Shaopeng Li,<sup>ab</sup> Yanyan Wang,<sup>ab</sup> Youdi Yang,<sup>ab</sup> Bingfeng Chen,<sup>a</sup> Jing Tai,<sup>c</sup> Huizhen Liu<sup>\*ab</sup> and Buxing Han<sup>\*ab</sup>

Herein, we demonstrate that quantum-sized Ru dots decorated ultra-thin anatase TiO<sub>2</sub> nanosheets with exposed (001) facets could exhibit the highly efficient catalytic activity for levulinic acid to  $\gamma$ -valerolactone at room temperature. The support effect has been largely attributed to the high energy of TiO<sub>2</sub> (001) which lead to stronger interaction between the support and the metal. The surface of Ru/TiO<sub>2</sub>-n contains more Ru (0) and result in higher activity and selectivity.

The nature of the support is very important for the supported metal catalysts. It has been widely recognized that the type of support could greatly affect the activity of the supported catalyst.<sup>1-6</sup> In recent years, it has been found that the activity and selectivity of the catalyst can also be affected by the same metal oxide support of different crystal forms.<sup>7-9</sup>

Nowadays, due to the large-scale use of fossil resources, the global warming problems such as air pollution and energy shortage become the world focus of constant attention. Therefore, the development of green renewable energy has become the focus of future research.<sup>10-13</sup> Biomass is the only renewable organic carbon resource in nature, which can be converted into fuel and chemical by biological transformation or chemical transformation, and thus partially replace fossil resources. Levulinic acid (LA) is one of the 12 most important platform compounds screened by the U.S. department of energy.<sup>14</sup> LA can be converted into a variety of high value-added derivatives, such as  $\gamma$ -valerolactone (GVL), angelica lactone (Al), 4-hydroxypentanoic acid (HPA), 1,4-pentanediol (PD) and methyltetrahydrofuran (MTHF).

GVL can be used as fuel additives, food ingredients, pharmaceutical intermediates, high-grade olefin green renewable fuels, solvents, nylon intermediates and other commercial purposes because of its excellent physical and

chemical properties, low toxicity and safe storage performance.<sup>15-20</sup>

The selective hydrogenation of LA to GVL has been studied widely. Ruthenium is considered as alternative active species for this process because of its good hydrogenation activity to the carbonyl compounds of aliphatic group.<sup>21-25</sup> On account that the nature of the support could affect the catalytic performance of the supported metal catalyst, the selective hydrogenation of LA to GVL over SiO<sub>2</sub>, Al<sub>2</sub>O<sub>3</sub>, active carbon and graphene supported Ru catalysts has been reported.<sup>26-29</sup> The groups of Bert M. Weckhuysen checked the influence of the support on catalyst selectivity and stability including Nb<sub>2</sub>O<sub>5</sub>, TiO<sub>2</sub> and H-ZSM5. The Ru/TiO<sub>2</sub> gave excellent selectivity to  $\gamma$ -valerolactone (GVL) (97.5%) at 100% conversion at 473K.<sup>30</sup> The groups of A. M. Ruppert investigated that the influence of different types of TiO<sub>2</sub> supports for ruthenium catalysts on the hydrogenation of levulinic acid towards  $\gamma$ -valerolactone.<sup>7</sup> They emphasize that the different electronic and surface properties of rutile and anatase can strongly affect the morphology and the activity of the catalysts.

It has been reported that the (001) surface of anatase TiO<sub>2</sub> has higher surface energy (0.90 J/m<sup>2</sup>) than the other surface.<sup>31-34</sup> It is possible to change the activity of Ru/TiO<sub>2</sub> by exposing different faces of TiO<sub>2</sub>. However, there have been no reports about the effect of different faces of support on the performance of the catalyst for the selective hydrogenation of LA to GVL.

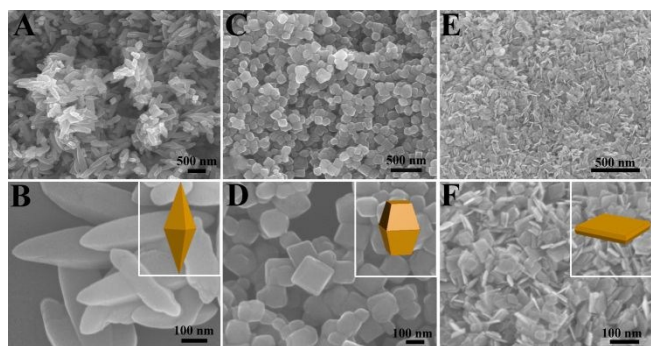
In this work, we prepared anatase-phase TiO<sub>2</sub> with different shapes including TiO<sub>2</sub> octahedron(TiO<sub>2</sub>-o), TiO<sub>2</sub> decanedron(TiO<sub>2</sub>-d) and TiO<sub>2</sub> nanosheet(TiO<sub>2</sub>-n). The catalytic activity of Ru/TiO<sub>2</sub>-o, Ru/TiO<sub>2</sub>-d and Ru/TiO<sub>2</sub>-n was investigated for the selective hydrogenation of LA to GVL, and found that Ru/TiO<sub>2</sub>-n exhibited the best catalytic performance. The yield of GVL can reach 99% at room temperature after 8 h over Ru/TiO<sub>2</sub>-n.

<sup>a</sup>Beijing National Laboratory for Molecular Sciences, CAS Key Laboratory of Colloid and Interface and Thermodynamics Institute of Chemistry, Chinese Academy of Sciences Beijing 100190 (P.R. China) E-mail: liuhz@iccas.ac.cn, hanbx@iccas.ac.cn

<sup>b</sup>University of Chinese Academy of Sciences, Beijing 100049, P. R. China

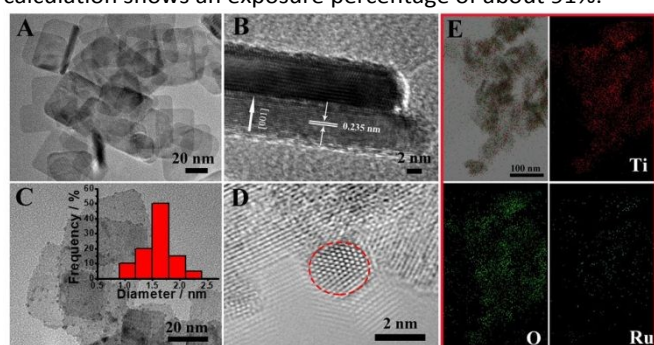
<sup>c</sup>Testing and Analysis Center, Institute of Chemistry, Chinese Academy of Sciences Beijing 100190 (P.R. China)

† Electronic Supplementary Information (ESI) available: Experimental procedure, and additional Figures. See DOI: 10.1039/x0xx00000x



**Fig. 1** SEM images with different magnifications of (A, B)  $\text{TiO}_2\text{-o}$ , (C, D)  $\text{TiO}_2\text{-d}$ , (E, F)  $\text{TiO}_2\text{-n}$ .

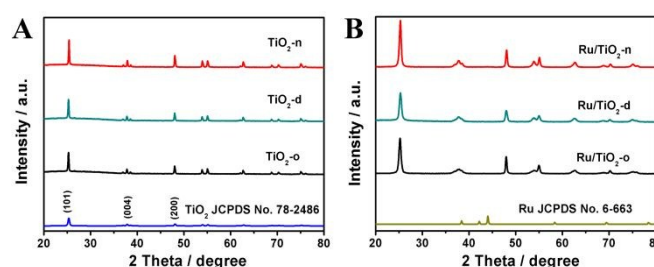
The typical scanning electron microscope (SEM) images of  $\text{TiO}_2\text{-x}$  ( $\text{TiO}_2\text{-o}$ ,  $\text{TiO}_2\text{-d}$  and  $\text{TiO}_2\text{-n}$ ) are shown in Fig. 1. As shown in the Fig. 1A and Fig. 1B, the typical octahedron of  $\text{TiO}_2$  has been successfully prepared and the average side length of ca. 300 nm and thickness of about 500 nm. The  $\text{TiO}_2\text{-o}$  has very few (001) faces leak out. The proportion of (001) facets as well as morphology of  $\text{TiO}_2$  nanoproducts could be tailored by simply adjusting the preparation methods. The decanedron bipyramid  $\text{TiO}_2$  structures (Fig. 1C and Fig. 1D) with an average side length of ca. 120 nm have been synthesized, which correspond to 14.9% facets exposed on the surface of  $\text{TiO}_2$ .<sup>35</sup> To get more of the (001) facets, the  $\text{TiO}_2$  nanosheets (Fig. 1E, Fig. 1F) with an average side length of ca. 40-70 nm and thickness of about 5 nm have been obtained. The geometric calculation shows an exposure percentage of about 91%.<sup>36</sup>



**Fig. 2** (A) TEM images of  $\text{TiO}_2$  nanosheets. (B) HRTEM image of  $\text{TiO}_2$  nanosheets. (C) TEM images of  $\text{Ru/TiO}_2$  nanosheets. (D) HRTEM images of Ru nanoparticles. (E) HAADF-STEM images and EDS elemental mapping images (Ti, O, and Ru elements) of the  $\text{Ru/TiO}_2$  nanosheets.

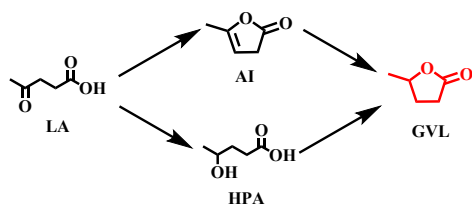
The typical transmission electron microscopy (TEM) images of  $\text{Ru/TiO}_2$  are shown in Fig. 2. The Fig. S1 is potassium titanate TEM image showing that the product contains a large quantity of nanowires with narrow size distribution. The diameters of the nanowires are uniform and around 10 nm and the lengths range from 500 nm up to 1 mm. Fig. 2A indicates that  $\text{TiO}_2\text{-n}$  support was synthesized with an average side length of ca. 40-70 nm. Fig. 2B shows the High-Resolution transmission electron microscopy (HRTEM) which the lattice spacing parallel to the top and bottom facets is 0.235 nm, corresponding to the (001) planes of anatase  $\text{TiO}_2$  crystals. Furthermore, Fig. 2C

shows the TEM images of the prepared  $\text{Ru/TiO}_2\text{-n}$ , in which the product consists of uniform Ru nanoparticles (NP) with spherical shape and an average diameter of  $1.8 \pm 1.0$  nm. The loading content of Ru was analyzed by inductively coupled plasma (ICP) mass spectrometry (Table S1 of the Supporting Information). The HRTEM images (Fig. 2D) clearly reveals that the lattice spacing of the Ru nanoparticles is ca. 0.20 nm, which is consistent with the lattice spacing of (101) plane of metallic Ru. The High-angle annular dark field scanning transmission electron microscopy (HAADF-STEM) images analysis reveals that the Ru nanoparticles are evenly dispersed on  $\text{TiO}_2$  (Fig. 2E). In energy-dispersive X-ray spectroscopy (EDS) mapping of the  $\text{Ru/TiO}_2\text{-n}$  catalyst, Ti, O, and Ru were detected, suggesting that all elements are evenly distributed. Furthermore, Fig. S2 shows the energy dispersive X-ray (EDX) result of  $\text{Ru/TiO}_2\text{-n}$  samples. It can be seen that except for the elements of Ti and O from the catalyst, the Ru elements were observed, indicating that Ru nanoparticles were successfully deposited on the  $\text{TiO}_2$  nanosheet. For comparison, the  $\text{Ru/TiO}_2\text{-o}$  and  $\text{Ru/TiO}_2\text{-d}$  catalysts also prepared by the same reduction process and the TEM images have also been shown in Fig. S3. The nanoparticles with an average diameter of 1.3 nm (inset of Fig. S3A) are immobilized uniformly on the  $\text{TiO}_2\text{-o}$ . The  $\text{Ru/TiO}_2\text{-d}$  include uniform spherical nanoparticles with an average diameter of 1.8 nm (inset of Fig. S3B). The TEM images of the commercial  $\text{TiO}_2$  ( $\text{Ru/TiO}_2\text{-com.}$ ) were also shown in Fig. S4. The Ru nanoparticles in these supported catalysts have similar particle sizes.



**Fig. 3** (A) XRD patterns of pristine (A)  $\text{TiO}_2\text{-n}$ ,  $\text{TiO}_2\text{-d}$ ,  $\text{TiO}_2\text{-o}$  and (B)  $\text{Ru/TiO}_2\text{-n}$ ,  $\text{Ru/TiO}_2\text{-d}$ ,  $\text{Ru/TiO}_2\text{-o}$ .

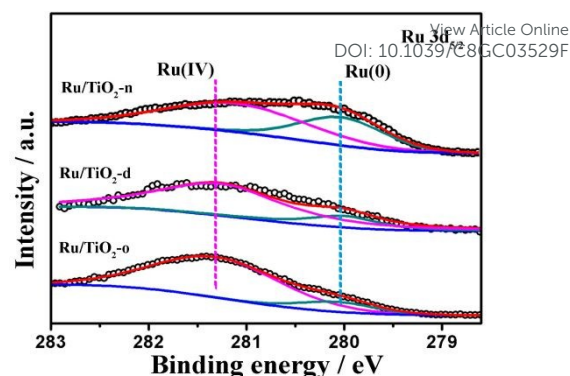
To further confirm the compositions of the catalyst, the X-ray diffraction (XRD) pattern has been performed and presented in Fig. 3. The diffraction peaks could be indexed to anatase-phase  $\text{TiO}_2$  (JCPDS No. 78-2486), indicating that the as synthesized product was pure anatase  $\text{TiO}_2$ . It is noteworthy that with increasing (001) crystal face amount of  $\text{TiO}_2\text{-o}$  and  $\text{TiO}_2\text{-d}$ , the XRD peak intensities of the samples steadily increase and the (001) peaks of the  $\text{TiO}_2$  nanosheets become enhanced. These phenomena indicate that more and more (001) of  $\text{TiO}_2$  is exposed. It was noteworthy that no obvious diffraction peaks of metallic Ru were observed in the  $\text{Ru/TiO}_2$  catalyst, which mainly because very small particles do not have long-range ordering to facilitate visible XRD peaks.

**Table 1. Catalytic Performance of Different Catalysts in the Hydrogenation of LA<sup>a</sup>**

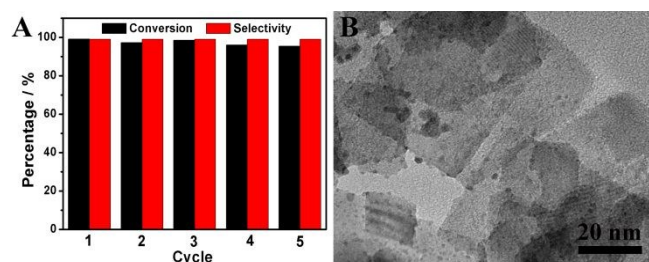
Entry	Catalysts	Time / h	Conversion <sup>b</sup> / %	Selectivity <sup>c</sup> / %			TOF <sup>d</sup> / h <sup>-1</sup>
				HPA	AI	GVL	
1	no	4	-	-	-	-	-
2	Ru/TiO <sub>2</sub> -n	8	>99	-	-	>99	41.5
3	Ru/TiO <sub>2</sub> -d	8	63	18.2	1.5	80.3	23.4
4	Ru/TiO <sub>2</sub> -o	8	54	25.2	2.0	72.8	12.8
5 <sup>e</sup>	Ru/TiO <sub>2</sub> -c	4	25	43.5	-	56.5	9.2
6	Ru/C	4	21	9.7	-	90.3	-
7 <sup>f</sup>	Ru/TiO <sub>2</sub> -n	4	-	-	-	-	-
8 <sup>g</sup>	Ru/TiO <sub>2</sub> -n	8	63	67.2	-	32.8	-
9 <sup>h</sup>	Ru/TiO <sub>2</sub> -n	8	28	-	-	>99	-
10 <sup>i</sup>	Ru/TiO <sub>2</sub> -n	8	-	-	-	-	-

<sup>a</sup>Reaction conditions: LA (1.0 mmol), H<sub>2</sub>O (2 mL), catalyst (20 mg), T (30 °C), P<sub>H<sub>2</sub></sub>(3 MPa), stirring speed (800 rpm). <sup>b</sup>Conversion of LA was determined by GC. <sup>c</sup>Selectivity of GVL was determined by GC. <sup>d</sup>TOF = mol of product/ mol of (Ru)×h<sup>-1</sup> (conversion of LA is less than 10%) <sup>e</sup>TiO<sub>2</sub>-c is commercial anatase TiO<sub>2</sub>. <sup>f</sup>Without H<sub>2</sub>. <sup>g</sup>methanol. <sup>h</sup> alcohol. <sup>i</sup>1,4-dioxane.

The hydrogenation and dehydration of LA was carried out in aqueous solutions (Table 1). In 4 hours, the conversion of LA was 65%, 41%, 32% for the Ru/TiO<sub>2</sub>-n, Ru/TiO<sub>2</sub>-d and Ru/TiO<sub>2</sub>-o, respectively (Fig. S5). More importantly, the selectivity of GVL was about 90% over Ru/TiO<sub>2</sub>-n. However, the selectivity of GVL is only 76.5%, 60.0% for Ru/TiO<sub>2</sub>-d and Ru/TiO<sub>2</sub>-o, the byproduct is AI and HPA. When the reaction time was extended to 8 hours, the yield of GVL could be 99% over Ru/TiO<sub>2</sub>-n, LA could completely transform into the desired products. However, In the same reaction conditions, Ru/TiO<sub>2</sub>-d and Ru/TiO<sub>2</sub>-o need more reaction time for the hydrogenation and dehydration of LA reaction, the conversion of LA and the selectivity of GVL were 63%/80.3% and 54%/72.8%, respectively (entry 3 and entry 4, Table 1). As a comparison, the conversion of GVL was only 25% over Ru/TiO<sub>2</sub>-com. under the same conditions for the hydrogenation and dehydration of LA (entry 5, Table 1). Surprisingly, the Ru/TiO<sub>2</sub>-n catalysts prepared in this work could catalyze the reaction very efficiently with the higher TOF (entry 2, Table 1). The commercial-Ru/C(Ru/C-com.) also showed poor catalytic activity (entry 6, Table 1). The reaction results of these catalysts proved that TiO<sub>2</sub>-n as support had high catalytic activity for hydrogenation of LA. When the hydrogen atmosphere absent, the GVL was not produced (entry 7, Table 1). This shows that hydrogen was indispensable. Furthermore, the influence of different solvent on the hydrogenation of LA was studied and the results were shown in Table 1(entry 8-10). It can be seen that methanol and alcohol exhibited very low conversion of LA(63%, 28%), respectively. There is almost no reaction in 1,4-dioxane solvent. H<sub>2</sub>O was the best solvent among the solvents we checked. The yield of GVL could reach 99% in H<sub>2</sub>O.

**Fig. 4** Ru 3d<sub>5/2</sub> XPS spectra of TiO<sub>2</sub>-supported Ru (Ru/TiO<sub>2</sub>-n, Ru/TiO<sub>2</sub>-d and Ru/TiO<sub>2</sub>-o).

In order to further study the interaction between metal and support. The XPS showed that the enhanced activity and stability of Ru/TiO<sub>2</sub>-n catalysts may be attributed to the interaction between Ru nanoparticles and TiO<sub>2</sub> nanosheet. Notwithstanding, the Ru 3d<sub>3/2</sub> signal interferes with the C 1s signal and thus is difficult to resolve. Ru 3d<sub>5/2</sub> was not affected by C 1s, so we measured Ru3d<sub>5/2</sub> to study the oxidation states of Ru. As shown in Fig. 4, the oxidation state of Ru metal was different in Ru/TiO<sub>2</sub>-n, Ru/TiO<sub>2</sub>-d and Ru/TiO<sub>2</sub>-o catalyst. The Ru 3d<sub>5/2</sub> binding energy of Ru/TiO<sub>2</sub>-o is 281.27 eV. The peak deconvolution indicates that the surface composition is 87.1% Ru (IV) and 12.9% Ru (0). The Ru 3d<sub>5/2</sub> binding energy of Ru/TiO<sub>2</sub>-d is 280.99 eV and the peak deconvolution indicates that the surface composition is 85.8% Ru (IV) and 14.2% Ru (0). These results show that Ru nanoparticles are easily oxidized. The other hand, the degree of oxidation is different on the different crystal surfaces. More interesting, the Ru 3d<sub>5/2</sub> binding energy of Ru/TiO<sub>2</sub>-n is 280.39 eV and the peak deconvolution indicates that the surface is composed of 61.8% Ru (IV) and 38.2% Ru (0). These results indicate that the surface of Ru/TiO<sub>2</sub>-n contains more Ru (0). It may be that the surface of TiO<sub>2</sub>-n has more defect sites, which leads to stronger metal interaction with the support. Because TEM already showed that the nanoparticles size of Ru are similar for Ru/TiO<sub>2</sub>-o, Ru/TiO<sub>2</sub>-d and Ru/TiO<sub>2</sub>-n catalyst. It means that higher activity is attributed to the presence of more surface Ru (0) for Ru/TiO<sub>2</sub>-n.

**Fig. 5** (A) Reusability of Ru/TiO<sub>2</sub>-n under the condition given as entries 1-4 in Table 1. (B) TEM images of the catalyst after cycling.

To verify the durability of the Ru/TiO<sub>2</sub>-n catalyst, the reusability was tested for the hydrogenation and dehydration of LA to GVL. After the reaction, the reaction mixture was

centrifuged and the solid Ru/TiO<sub>2</sub>-n catalyst was recovered, followed by rinsing with THF and centrifugation (3×30 mL). The Ru/TiO<sub>2</sub>-n catalyst was reused directly for the next run after drying at 60 °C for 12 h in a vacuum oven. The results in Fig. 5A clearly showed that the catalysts can be used at least 5 times without obvious decrease in the conversion of LA and the reaction selectivity. The TEM image of the Ru/TiO<sub>2</sub>-n after used 5 times is shown in Fig. 5B. It can be seen that the Ru nanoparticles didn't aggregate compared with the virgin catalyst.

In summary, we have demonstrated a facile and efficient strategy for facilitating the GVL from LA by using quantum-sized Ru dots decorated ultra-thin anatase TiO<sub>2</sub> nanosheets as the catalysts under mild conditions. The support effect has been largely attributed to the high energy of TiO<sub>2</sub> (001) which leads to the stronger interaction of the Ru nanoparticles and the support. More Ru (0) is important for the improving activity of the Ru/TiO<sub>2</sub>-n. The results could also provide helpful insights for the efficient catalyst for the other reaction using high energy support.

### Conflicts of interest

The authors declare no conflicts of interest.

### Acknowledgements

This work was supported by the National Key Research and Development Program of China (2018YFB0605801, 2017YFA0403103), National Natural Science Foundation of China (21603235), Chinese Academy of Sciences (QYZDY-SSW-SLH013), the Recruitment Program of Global Youth Experts of China.

### Notes and references

- N. Ta, J. J. Liu, S. Chenna, P. A. Crozier, Y. Li, A. Chen and W. Shen, *Journal of the American Chemical Society*, 2012, **134**, 20585-20588.
- D. Zhao, Q. Huo, J. Feng, B. F. Chmelka and G. D. Stucky, *Journal of the American Chemical Society*, 2014, **136**, 10546-10546.
- W. Jiang, B. Xu, Z. Xiang, X. Liu and F. Liu, *Applied Catalysis A: General*, 2016, **520**, 65-72.
- S. Wu, Q. He, C. Zhou, X. Qi, X. Huang, Z. Yin, Y. Yang and H. Zhang, *Nanoscale*, 2012, **4**, 2478-2483.
- J. Lee, J. C. Park and H. Song, *Advanced Materials*, 2008, **20**, 1523-1528.
- G. Chen, R. Gao, Y. Zhao, Z. Li, G. I. N. Waterhouse, R. Shi, J. Zhao, M. Zhang, L. Shang, G. Sheng, X. Zhang, X. Wen, L. Z. Wu, C. H. Tung and T. Zhang, *Adv Mater*, 2018, **30**.
- A. M. Ruppert, J. Grams, M. Jedrzejczyk, J. Matras-Michalska, N. Keller, K. Ostojka and P. Sautet, *ChemSusChem*, 2015, **8**, 1538-1547.
- C. Liu, X. Han, S. Xie, Q. Kuang, X. Wang, M. Jin, Z. Xie and L. Zheng, *Chemistry, an Asian journal*, 2013, **8**, 282-289.
- F. Wang, H. Z. Wu, C. L. Liu, R. Z. Yang and W. S. Dong, *Carbohydrate research*, 2013, **368**, 78-83.
- J. Q. Bond, D. M. Alonso, D. Wang, R. M. West and J. A. Dumesic, *Science*, 2010, **327**, 1110-1114.
- C.-H. Zhou, X. Xia, C.-X. Lin, D.-S. Tong and J. Beltrami, *Chemical Society Reviews*, 2011, **40**, 5588-5617.
- J. Q. Bond, A. A. Upadhye, H. Olcay, G. A. Tompsett, J. Jae, R. Xing, D. M. Alonso, D. Wang, T. Zhang, R. Kumar, A. Foster, S. M. Sen, C. T. Maravelias, R. Malina, S. R. H. Barrett, R. Lobo, C. E. Wyman, J. A. Dumesic and G. W. Huber, *Energy & Environmental Science*, 2014, **7**, 1500-1523.
- B. Girisuta, L. Janssen and H. J. Heeres, *Industrial & Engineering Chemistry Research*, 2007, **46**, 1696-1708.
- J. J. Bozell and G. R. Petersen, *Green Chemistry*, 2010, **12**, 539-554.
- W. R. H. Wright and R. Palkovits, *ChemSusChem*, 2012, **5**, 1657-1667.
- W. Li, J.-H. Xie, H. Lin and Q.-L. Zhou, *Green Chemistry*, 2012, **14**, 2388-2390.
- J. Q. Bond, D. M. Alonso, R. M. West and J. A. Dumesic, *Langmuir*, 2010, **26**, 16291-16298.
- S. G. Wettstein, D. M. Alonso, Y. Chong and J. A. Dumesic, *Energy & Environmental Science*, 2012, **5**, 8199-8203.
- F. D. Pileidis and M.-M. Titirici, *ChemSusChem*, 2016, **9**, 562-582.
- P. J. Deuss, K. Barta and J. G. de Vries, *Catalysis Science & Technology*, 2014, **4**, 1174-1196.
- A. M. R. Galletti, C. Antonetti, V. De Luise and M. Martinelli, *Green Chemistry*, 2012, **14**, 688-694.
- P. P. Upare, J.-M. Lee, D. W. Hwang, S. B. Halligudi, Y. K. Hwang and J.-S. Chang, *Journal of Industrial and Engineering Chemistry*, 2011, **17**, 287-292.
- C. Michel, J. Zaffran, A. M. Ruppert, J. Matras-Michalska, M. Jedrzejczyk, J. Grams and P. Sautet, *Chemical Communications*, 2014, **50**, 12450-12453.
- Z.-p. Yan, L. Lin and S. Liu, *Energy & Fuels*, 2009, **23**, 3853-3858.
- B. Coq, A. Bittar and F. Figueras, *Applied Catalysis*, 1990, **59**, 103-121.
- M. G. Al-Shaal, W. R. H. Wright and R. Palkovits, *Green Chemistry*, 2012, **14**, 1260-1263.
- C. Xiao, T.-W. Goh, Z. Qi, S. Goes, K. Brashler, C. Perez and W. Huang, *Acs Catalysis*, 2016, **6**, 593-599.
- S. Ishikawa, D. R. Jones, S. Iqbal, C. Reece, D. J. Morgan, D. J. Willock, P. J. Miedziak, J. K. Bartley, J. K. Edwards, T. Murayama, W. Ueda and G. J. Hutchings, *Green Chemistry*, 2017, **19**, 225-236.
- W. Luo, M. Sankar, A. M. Beale, Q. He, C. J. Kiely, P. C. A. Bruijninx and B. M. Weckhuysen, *Nature Communications*, 2015, **6**.
- W. Luo, U. Deka, A. M. Beale, E. R. H. van Eck, P. C. A. Bruijninx and B. M. Weckhuysen, *Journal of Catalysis*, 2013, **301**, 175-186.
- X. Q. Gong and A. Selloni, *Journal of Physical Chemistry B*, 2005, **109**, 19560-19562.
- F. De Angelis, G. Vitillaro, L. Kavan, M. K. Nazeeruddin and M. Graetzel, *Journal of Physical Chemistry C*, 2012, **116**, 18124-18131.
- A. Selloni, *Nature Materials*, 2008, **7**, 613-615.
- S. Li, H. Hu and Y. Bi, *Journal of Materials Chemistry A*, 2016, **4**, 796-800.
- C. Liu, X. Han, S. Xie, Q. Kuang, X. Wang, M. Jin, Z. Xie and L. Zheng, *Chemistry-an Asian Journal*, 2013, **8**, 282-289.

## Journal Name

COMMUNICATION

36. L. Q. Ye, J. Mao, J. Y. Liu, Z. Jiang, T. Y. Peng and L. Zan, *Journal of Materials Chemistry A*, 2013, **1**, 10532-10537.

View Article Online  
DOI: 10.1039/C8GC03529F

Green Chemistry Accepted Manuscript



View Article Online

DOI: 10.1039/C8GC03529F

Shaopeng Li,<sup>ab</sup> Yanyan Wang,<sup>ab</sup> Youdi Yang,<sup>ab</sup> Bingfeng Chen,<sup>a</sup> Jing  
Tai,<sup>c</sup> Huizhen Liu<sup>\*ab</sup> and Buxing Han<sup>\*ab</sup>

**Conversion of levulinic acid to  $\gamma$ -valerolactone over  
ultra-thin  $\text{TiO}_2$  nanosheets decorated with ultras-small Ru  
nanoparticle catalysts under mild condition**